Fiore, G., Perrino, G., Di Bernardo, M., & di Bernardo, D. (2015). *In Vivo* Real-Time Control of Gene Expression: A Comparative Analysis of Feedback Control Strategies in Yeast. *ACS Synthetic Biology*, *5*(2), 154-162. https://doi.org/10.1021/acssynbio.5b00135

In-vivo real-time control of gene expression: a comparative analysis of feedback control strategies in yeast

Gianfranco Fiore,[†,‡,§] Giansimone Perrino,[†,‡,§] Mario di Bernardo,[*,‡,¶] and Diego di Bernardo[*,†,‡]

TeleThon Institute of Genetics and Medicine (TIGEM), Pozzuoli, Italy, Department of Electrical Engineering and Information Technology, University of Naples Federico II, Naples, Italy, and Department of Engineering Mathematics, University of Bristol, Bristol, UK

E-mail: mario.dibernardo@unina.it; dibernardo@tigem.it

Abstract

Real-time automatic regulation of gene expression is a key technology for synthetic biology enabling, for example, synthetic circuit's components to operate in an optimal range. Computer-guided control of gene expression from a variety of inducible promoters has been only recently successfully demonstrated. Here we compared, *in-silico* and *in-vivo*, three different control algorithms: the Proportional-Integral (PI) and Model Predictive Control (MPC) controllers, which have already been used to control gene expression, and the Zero Average Dynamics (ZAD), a control technique used to regulate

[*]To whom correspondence should be addressed
[†]TIGEM
[‡]University of Naples Federico II
[¶]University of Bristol
[§]These authors contributed equally to this work

electrical power systems. We chose as an experimental test-bed the most commonly used inducible promoter in yeast: the Galactose-responsive *GAL1* promoter. We set two control tasks: either force cells to express a desired constant fluorescence level of a reporter protein downstream of the *GAL1* promoter (set-point), or a time-varying fluorescence (tracking). Using a microfluidics-based experimental platform, in which either glucose or galactose can be provided to the cells, we demonstrated that both the MPC and ZAD control strategies can successfully regulate gene expression from the *GAL1* promoter in living cells for thousands of minutes. The MPC controller can track fast reference signals better than ZAD, but with an higher actuation effort due to the large number of input switches it requires. Conversely the PI controller's performance is comparable to that achieved by the MPC and the ZAD controllers only for the set-point regulation.

Keywords

synthetic biology, control engineering, microfluidics, gene expression, yeast

Control Engineering aims at driving a physical system in order to attain a specific value of a quantity of interest (such as a boiler that needs to warm water to a desired temperature, or a car cruise-control maintaining a constant speed) despite the presence of disturbances. This is achieved by appropriately varying its inputs (switch on or off a heater in the case of the boiler, or accelerating or braking in the cruise-control) as a function of the difference between the measured value of the output and its desired target value (control error). At the core of most control schemes lies a *negative feedback* loop (*1*), as shown in Figure 1 - A. The variable to be controlled (system output y) is measured and its value is subtracted from the desired value (control reference r). The quantity that is obtained, the control error

e, is minimised by the controller, a set of logical and mathematical rules through which an appropriate value of the input u is chosen in order to guarantee that the output y matches the desired reference r.

Feedback control has been extensively applied to control growing conditions of cells in chemostats in terms of temperature and/or CO2 and it is a current feature of bench-top and industrial chemostats (*2*, *3*). Only recently, however, the application of Control Engineering principles has been exploited to regulate molecular events in living cells, thanks to innovative microfludics and optogenetics platforms (*4*–*8*).

In (*4*, *5*) we built a completely automated microfluidic platform to control in real-time gene expression in yeast cells. We demonstrated the ability of the platform to reach and maintain a desired value of gene expression, measured in terms of the fluorescence intensity of a reporter protein expressed from the endogenous *GAL1* promoter.

Other successful attempts to control gene expression, or even signaling pathways, have been described in the literature. They mainly differ in the control input (osmotic pressure, light, small-molecules) and the control strategy adopted. Optogenetics-based light inducible systems have been exploited to control gene expression in yeasts (*8*, *9*), to regulate intracellular signalling dynamics in mammalian cells (*7*), and to drive protein levels by using light-switchable two-component systems in bacteria (*10*). Microfluidic-based devices, allowing a tight control of cellular growing medium and the administration of inducer small-molecules, have been successfully employed to investigate synchronisation properties of synthetic biological clocks in bacterial cells (*11*), to control the transcription from the *HOG1* promoter in yeast *S. Cerevisiae* by varying the osmotic pressure(*6*) and, in our own work, to control transcription from the *GAL1* promoter using Galactose and Glucose as input.

The different control strategies proposed in the literature have never been compared in the same experimental model, thus making a direct comparison of their performance impossible. This is extremely important for practical applications where knowing advantages and limitations of each strategy can be useful, if not necessary, to select the most appropriate

and effective one. Here, we compared *in-silico* and *in-vivo* the performance of different control algorithms when applied to the problem of controlling gene expression from the *GAL1* inducible promoter. In addition to control strategies that have already been described in the literature, namely the Proportional-Integral (PI) control and the Model Predictive Control (MPC), we also tested a different control strategy named Zero Average Dynamics (ZAD), an approach inspired by sliding control techniques (*12*) used to control power electronic systems, but that has never been applied to biological processes. Finally, practical considerations of the pros and cons of each control strategy are provided.

Results and Discussion

An experimental testbed for the assessment of control strategies.

The *GAL1* promoter is the most widely used inducible promoter in yeast genetics. Thousands of strains, each expressing a different yeast gene, are available to the research community, making this an attractive choice for practical applications of control engineering. The activity of the *GAL1* promoter is governed by the presence of Galactose in the cells' growing medium. This sugar is interpreted as a "switch on" signal for the expression of the *GAL1* gene; when yeasts are fed with Glucose, the production of Gal1 protein is repressed (*13*). Yeast cells will first consume all the available Glucose in the medium before starting metabolising Galactose. Hence, the control input can either be Glucose (switch off signal) or Galactose (switch on signal), but not an intermediate concentration of the two, because cells will not respond to Galactose when Glucose is present.

We thus decided to use the *GAL1* promoter upstream of a reporter gene (Gfp fused with the Gal1 protein) as a testbed for comparing and assessing the performance of the different control strategies. When dealing with living cells, one of the major issues is represented by the uncertainty affecting transcriptional and translational processes, introducing a remarkable cell-to-cell variability in mRNA and protein production (*14*). Rather than trying to control

stochastic behaviour of cells, here we addressed the simpler problem of regulating the average fluorescence intensity expressed by all cells as the quantity to be controlled (y), thus averaging out the effects due to intrinsic and extrinsic sources of noise (*15*).

To carry out *in-vivo* control experiments, we used the same integrated experimental set-up presented in previous works (*5*, *16*), comprising a microfluidic device, a time-lapse microscope, and a set of automated syringes, all controlled by a computer. As depicted in Figure 1 - B, the computer runs the control algorithm, which at each sampling interval: *(i)* processes images acquired by the microscope to estimate the fluorescence y; *(ii)* executes the control algorithm to derive the input u for the next sampling period; *(iii)* controls the automated syringes to provide the calculated input (i.e. Galactose or Glucose) to the cells. We already demonstrated that the average fluorescence level of a yeast population can be effectively regulated with this platform using a simple Proportional-Integral control strategy(*5*).

Controlling gene expression from the *GAL1* promoter: set-point and tracking control tasks.

We compared the performance of three control algorithms (PI, MPC and ZAD) when performing two different tasks, as shown Figure 2: *(i) set-point control*, where the average Gfp fluorescence must reach and maintain a desired reference level, and *(ii) signal tracking control* where the average fluorescence must follow (or track) a desired time-varying signal. Specifically, in the **set-point control** (Figure 2 - A), the desired fluorescence r was set equal to 50% of the initial average fluorescence expressed by the cells during the calibration phase of 180 min. During the calibration phase, cells are kept in Galactose, in order to let cells adapt to the microfluidic environment, and to set the unit of measure of fluorescence, which may vary due to technical and biological variability in each experiment. In the **signal tracking control**, we used three different references r: *(i)* a descending staircase function (Figure 2 - B) where each step lasts 500 min, beginning at 75% of the calibration phase average flu-

orescence, then stepping down to 50% and then 25%, *(ii)* a linear descending ramp of 1500 min (Figure 2 - C) starting at the 100% of average fluorescence measured in the calibration phase, and decreasing down to 25%, and *(iii)* a sinusoidal wave of period $T = 2000$ min (Figure 2 - D) defined as $s(t) = 0.5 + 0.25 \sin\left(\frac{2\pi}{T}(t - 100) + \frac{\pi}{2}\right)$.

Control algorithms.

PI and MPC have been previously applied to control gene expression and protein activation. Toettcher and colleagues applied a Proportional-Integral (PI) control to regulate protein signaling in mammalian cells using light as control input in an optogenetics framework(*7*); we have applied the same PI control scheme to regulate gene expression from the *GAL1* promoter in yeast using galactose and glucose as control input(*5*); Milias et al (*8*) implemented MPC to control expression from the *GAL1* promoter in yeast using light as a control input to activate transcription. The same MPC strategy was also applied by Uhlendorf et al (*6*) to control expression from the *HOG1* promoter in yeast using osmotic pressure as the control input.

We therefore compared the performance of PI, MPC and a new ZAD controller when applied to the regulation of gene expression from the *GAL1* promoter in yeast cells.

We identified two major constraints affecting the control algorithms: the sampling-time and the admissible values of the control input. We set the sampling time $T = 5\ min$, this is the time interval at which images are acquired from the microscope and it is an ideal trade off to avoid photo-toxicity and capture the dynamics of the Gfp protein expression (*17*). The control input u can assume only two values (Galactose-ON, Glucose-OFF). Thus, at each sampling time kT, the control algorithms can only choose the duration of Galactose pulse (ON), which can vary from 0 min to 5 min, and it is defined as the duty-cycle $d = \frac{t_{ON}}{T}$, i.e. the percentage of the time interval during which Galactose is provided to the cells.

The Proportional-Integral (PI) control algorithm uses the *control error* $e(t) = r(t) - y(t)$ to choose, at each sampling time (kT), the duty-cycle value (d_k). Specifically d_k has a value

proportional to the weighted sum of two contributions, one proportional to the actual error $e(t)$ and the other proportional to the sum of the past values of the error (the integral term). The proportionality constants K_p and K_i are called respectively proportional and integral gains, and their values were chosen by simple empirical rules (Methods and Supporting Informations) (*1*).

The Model Predictive Control (MPC) algorithm is an optimisation-based technique which uses a mathematical model of the process being controlled to predict the future values of the control error and to find the best value of the duty-cycle value d_k that minimises it (Methods and Supporting Informations) (*18*).

The Zero Average Dynamics (ZAD) algorithm relies on a feedback strategy devised for the regulation of power converters (*19*, *20*), it is a modified version of Sliding Mode Control (*12*). Specifically, the ZAD calculates, at each sampling time, the best value of d_k which minimises the actual control error $e(t)$ and its predicted future value (estimated by the derivative $\dot{e}(t)$) over the next time interval (refer to Methods section and Supporting Informations for further details).

Set-point control experiments

We first tested *in-silico* the PI, MPC and ZAD control strategies described above, by simulating the behaviour of yeast cells in a computer (Methods and Supporting Informations). *In-silico* results are shown in Figure 3. PI (Figure 3 A), MPC (Figure 3 B) and ZAD (Figure 3 C) are able to reach and maintain the desired fluorescence value without exhibiting oscillations at steady-state. Performance indexes (ISE, IAE, ITAE in Figure 3 D) are of the same order of magnitude for all the control strategies; interestingly the ZAD controller is able to achieve satisfying results with a reduced number of input switches (five and six fold less than respectively MPC and PI). This is advantageous in the experimental setting because it reduces unnecessary stress to cells.

In-vivo control experiments, shown in Figure 4, mirror *in-silico* results, showing that the three strategies are indeed all able to reach and maintain the desired fluorescence level. As predicted by the *in-silico* simulations, the ZAD controller employs fewer Galactose pulses (Figure 4 C) and displays smaller oscillations around the set-point than the MPC feedback strategy (Figure 4 B).

Signal tracking control experiments

In-silico simulation of the descending staircase reference shows that the three control strategies have different performances. The PI is not able to properly follow the reference signal (Figure 5 A). This is to be expected, since the PI controller was designed specifically to solve set-point control tasks (*1*). The MPC control algorithm, with its intrinsic predictive ability, achieves a good performance, specifically noticeable in the proximity of the steps' edges (Figure 5 B). Indeed, the MPC is able to foresee changes in the reference signal and to adjust the control input accordingly, by starting to "switch off" the system in advance. The ZAD control algorithm (Figure 5 C) achieves satisfying results, comparable to the MPC controller (except in the proximity of the steps' edges), but with a smaller number of Galactose pulses.

In-vivo experiments for the descending staircase reference (Figure 6) confirm *in-silico* results. The PI controller (Figure 6 A) poorly tracks the reference r, despite the high number of input switches. The MPC, as already demonstrated *in-silico*, has a much better performance, quantitatively confirmed by the performance indexes (Figure 6 B and D). As in the case of the *in-silico* simulations, the ZAD controller (Figure 6 B and D) achieves a performance comparable to that of the MPC (even if not as good in the proximity of the steps' edges) employing fewer Galactose pulses than the MPC.

Because of the poor tracking results achieved by the PI controller, we further compared only the MPC and ZAD controllers when tracking the ramp and the sinusoidal signal. Both *in-silico* (Figure 7) and *in-vivo* (Figure 8) observations confirm that the ZAD controller is able to guarantee a performance (Figure 7 E and Figure 8 E) similar to that of the MPC

strategy, but again with a reduced number of control input switches.

Conclusions

Precise and quantitative regulation of gene expression from inducible promoters is a key technology for current and future Synthetic Biology applications. It can be used to quantitatively characterise biological "parts" in a single experiment by generating a desired time-varying concentration of an effector protein and measuring the activity of the target. For example, the level of a Transcription Factor can be controlled to follow a descending staircase reference while, at the same time, measuring the level of a report protein downstream of the promoter to be characterised, in order to derive a quantitative dose-response curve to be used for modelling. A second application of automatic control of gene expression is to ensure that a synthetic circuit works in the optimal operating conditions in terms of expression of its constituent proteins, similarly to what happens in a modern computer where the operating temperature is automatically controlled by switching on/off a fan in order to keep the electronic circuits from overheating.

Here we provided a comparative analysis, *in-silico* and *in-vivo*, of three different strategies to control gene expression from the *GAL1* inducible promoter, whose advantages and disadvantages are summarised in Table 1.

To this end we implemented and compared PI and MPC controllers, which have been previously reported in the literature (*4–8*) and proposed an additional strategy, the ZAD controller (*19*).

We demonstrated that both MPC and ZAD control strategies can be successfully employed to control gene expression from the *GAL1* promoter to generate any desired time-varying concentration of the reporter protein. These controllers require a quantitative model of the system to be controlled. This is not a strong limitation, since it is possible to identify a dynamical input-output model of the biological system under investigation using standard system identification techniques, which work very well at least for simple inducible promoters

(*16*).

The PI controller, as expected from control theory (*1*) and from our *in-silico* predictions, performs similarly to the MPC and ZAD strategies only in the set-point control task, whereas it is the worst performer in the case of signal-tracking experiments.

The MPC and ZAD controller perform similarly well in all the control tasks. The main differences are that the MPC performs slightly better than ZAD for fast switching reference signals (such at the staircase signal in Figure 6), however it requires a higher number of input switches when compared to the ZAD controller. The ZAD technique may be advantageous in those applications in which a high cost is associated to the actuation such as when the input administration can cause stress to the cells (e.g light stimuli, antibiotic, osmotic shocks etc.).

In conclusion, automatic control of gene expression from inducible promoters is mature enough to be applied routinely in synthetic biology and more generally in quantitative biology applications. Although we showed the experimental application of these control strategies to the *GAL1* promoter, the same techniques can be applied to other inducible promoters and to different cellular models.

The choice of the control strategy to employ will depend on which kind of control task needs to be achieved (set-point or tracking), the complexity of the synthetic circuit to be controlled, the availability of a descriptive mathematical model of the circuit to be controlled, the cost associated to the actuation effort and, whether a minimal stress to the cells is required (i.e. a small number of input switches).

Table 1: Comparative analysis summary

Control Strategy	Model required	Pros	Cons
PI	No	⋆Robust ⋆Reduced computational complexity	−Not suitable for signal tracking control
MPC	Yes	⋆Suitable for set-point and signal tracking control ⋆Best performance for fast varying references	−High number of input switches
ZAD	Yes	⋆Suitable for set-point and signal tracking control ⋆Reduced number of input switches	−Performs slightly worse than MPC on fast varying references

Methods

Yeast strain and cell culture

Control experiments were performed in the yeast strain (yGIL337, Gal1-GFP::KanMX, Gal10-mCherry::NatMX) provided to us by Lang et al. (*21*). In this strain the Gal1 protein, expressed by the *GAL1* promoter, was fused to a green fluorescent protein (Gfp). Before each *in-vivo* control experiment started, cells were inoculated overnight in 10 mL synthetic complete medium + Galactose/raffinose (2%); the culture was then repeatedly diluted to achieve a final OD_{600} of 0.01 on the day the cells were injected into the microfluidic device (Supporting Informations for further details).

Microfluidics

The MFD0005a device was used for all the microfluidcs experiments(*17*). This device houses a micro-chamber (height: $3.5\mu m$) which "traps" yeast cells, that can only grow in a monolayer, thus allowing easier automated image analysis. Microfludics devices were fabricated as described in(*17*). Details of the microfludics set-up and of the galactose and glucose growing

medium used in the experiments can be found in (*5*) and Supporting Informations.

Microscopy and image analysis

To monitor cellular processes dynamics, as well as, to check for the right administration of external inputs to trapped cells, we took advantage of an inverted fluorescence microscope (Nikon Eclipse Ti) equipped with an automated and programmable stage, an incubator to guarantee fixed temperature and gasses to cell environment and a high sensitivity Electron Multiplying CCD (EMCCD) Camera (Andor iXON Ultra897). The microscope and the camera were programmed to acquire, at 5 min intervals, two types of images: *(a)* a bright field image (phase contrast) and *(b)* fluorescence images (with the appropriate filters) to monitor cell fluorescence and to track the dye (sulforhodamine) added to the inducer compound in order to evaluate the control input administered to the cells. Fluorescence was quantified using a previously developed custom image processing algorithm (*5*). The algorithm is able to locate cells within each Phase Contrast image thus identifying all pixels belonging to the cells. This information is used to calculate the fluorescence being expressed by the entire population as well as by each single cell. The actual measured fluorescence is mainly affected by the efficiency of the fluorescent lamp, and by the background light in the surrounding microscope environment. We observed that as the fluorescent lamp nears its life-time, its brightness decreases and this affects the measured fluorescence in the cells. Indeed, the measurement units for the fluorescence are considered arbitrary and, thus, a calibration phase at the beginning of each experiment is needed to calculate a reference value for the fluorescence.

Control strategies implementation

The control input is described as follows, where ON means galactose administration and OFF glucose administration:

$$u(t) = \begin{cases} u_{MAX} = ON & kT \leq t < (k + d_k)\, T \\ u_{MIN} = OFF & (k + d_k)\, T \leq t < (k + 1)\, T \end{cases} \tag{1}$$

PI: Proportional and integral gains, K_p and K_i were calculated with the Ziegler-Nichols' open-loop tuning method (*1*) applied to the mathematical model of the *GAL1* promoter described in the Supporting Informations. Thus the gains were set to $K_p = 13.49$ and $K_i = 0.17$.

Given the constraints on the control input as well as on the sampling time described above, a modulation on the PI output was implemented to calculate the duty cycle d_k as:

$$d_k = \frac{\hat{u} - u_{MIN}}{u_{MAX} - u_{MIN}}. \tag{2}$$

where $\hat{u}$ is the output of the PI regulator saturated between $u_{MIN} = 0$ and $u_{MAX} = 2$. To avoid delays and overshoots introduced by the saturation of the regulator output (*1*) an anti-windup block, described in the Supporting Informations, was added to the feedback loop.

MPC: The MPC strategy chooses, at each sampling time kT, the optimal control input that minimises the sum of the squared control error (SSE):

$$SSE \triangleq \sum_{i=k+1}^{k+N} \left(N + 1 + k - i\right) \epsilon_i^2 \quad = \sum_{i=k+1}^{k+N} \left(N + 1 + k - i\right) \left(\hat{y}_i - r_i\right)^2 \tag{3}$$

where $\hat{y}$ is the output provided by the dynamical model of the the *GAL1* promoter (Supplementary Information), which is computed by a Kalman state estimator, able to reconstruct system states from the measured output y, as shown Figure 1 - A. The integer $N = 12$ (corresponding to 60 min) defines the length of the prediction horizon in terms of sampling intervals. The forgetting factor $(N + 1 + k - i)$ weights the error samples more at the beginning of the prediction horizon than at the end; this guarantees faster corrections

of output deviations from the reference. The optimisation was carried out by adopting the Matlab implementation of the Genetic Algorithm described in (*22*).

The result of the optimisation is an array of N optimal duty cycles $d_{k+i}, i \in [1, N]$. In the absence of external disturbances and other sources of uncertainty, the optimal input computed by the MPC could, in principle, be applied to the yeast cells over the entire prediction horizon. However, in order to make the control action robust to any source of uncertainty and variability, the feedback loop is closed by applying only the first element of the calculated control input and at the next sampling time $(k+1)\,T$ when the entire procedure is repeated.

ZAD: Zero Average Dynamics (ZAD) control relies on a feedback strategy devised for the regulation of power converters and allows to directly calculate the duty cycle d_k of a switching control input (*19*, *23*). ZAD control is a practical implementation of sliding mode control (*12*), where the control objective consists in attracting and then maintaining onto a fixed surface $s(x) = 0$ (denoted as the sliding surface) the states of the system by appropriately switching the available inputs.

In the ZAD control approach, the sliding condition has to be fulfilled only on average over each sampling period kT, thus allowing to directly calculate the duty cycle d_k via the solution of the following integral equation:

$$\mathbb{E}_T\big[s\big(x(t)\big)\big] \;=\; \frac{1}{T}\int_{kT}^{(k+1)\,T} s\big(x(t)\big)\,dt \;=\; 0 \tag{4}$$

where $mathbbE_T$ indicates the operator taking the average over the time interval T.

To control *GAL1* promoter dynamics onto the desired reference signal, we considered the following sliding surface, which was derived using the dynamical model of the *GAL1* promoter as described in the Supplementary Information:

$$s\big(x(t)\big) \;=\; \big(x_2(t) - x_{2_{ref}}(t)\big) + \big(\dot{x}_2(t) - \dot{x}_{2_{ref}}(t)\big) \tag{5}$$

where x_2 is the state variable describing the dynamics of the fluorescent reporter note that $\dot{x}_{2_{ref}}(t) = 0$ in the case of set-point regulation.

For further details on the implementation of the ZAD controller refer to Supporting Informations.

Supporting Informations

Additional text and figures referenced in this article.

Acknowledgements

We are thankful to Prof. Botstein for providing yeast strains and Prof. Jeff Hasty for microfluidic device.

Funding sources

This work was supported by a Human Frontier Science Program HFSP RGP0020/2011 to DdB and by the Italian Fondazione Telethon.

References

1. Aström, K. J., and Murray, R. M. *Feedback systems: an introduction for scientists and engineers*; Princeton University Press, 2010.

2. Foss, B. A., Johansen, T. A., and Sørensen, A. V. (1995) Nonlinear predictive control using local models applied to a batch fermentation process. *Control Engineering Practice 3*, 389–396.

3. Liu, C., Gong, Z., Shen, B., and Feng, E. (2013) Modelling and optimal control for a fed-batch fermentation process. *Applied Mathematical Modelling 37*, 695–706.

4. Menolascina, F., di Bernardo, M., and di Bernardo, D. (2011) Analysis, design and implementation of a novel scheme for in-vivo control of synthetic gene regulatory networks. *Automatica 47*, 1265–1270.

5. Menolascina, F., Fiore, G., Orabona, E., De Stefano, L., Ferry, M., Hasty, J., di Bernardo, M., and di Bernardo, D. (2014) In-Vivo Real-Time Control of Protein Expression from Endogenous and Synthetic Gene Networks. *PLoS Computational Biology 10*, e1003625.

6. Uhlendorf, J., Miermont, A., Delaveau, T., Charvin, G., Fages, F., Bottani, S., Batt, G., and Hersen, P. (2012) Long-term model predictive control of gene expression at the population and single-cell levels. *Proceedings of the National Academy of Sciences 109*, 14271–14276.

7. Toettcher, J. E., Gong, D., Lim, W. A., and Weiner, O. D. (2011) Light-based feedback for controlling intracellular signaling dynamics. *Nature methods 8*, 837–839.

8. Milias-Argeitis, A., Summers, S., Stewart-Ornstein, J., Zuleta, I., Pincus, D., El-Samad, H., Khammash, M., and Lygeros, J. (2011) In silico feedback for in vivo regulation of a gene expression circuit. *Nature biotechnology 29*, 1114–1116.

9. Melendez, J., Patel, M., Oakes, B. L., Xu, P., Morton, P., and McClean, M. N. (2014) Real-time optogenetic control of intracellular protein concentration in microbial cell cultures. *Integrative Biology 6*, 366–372.

10. Olson, E. J., Hartsough, L. A., Landry, B. P., Shroff, R., and Tabor, J. J. (2014) Characterizing bacterial gene circuit dynamics with optically programmed gene expression signals. *Nature methods 11*, 449–455.

11. Danino, T., Mondragón-Palomino, O., Tsimring, L., and Hasty, J. (2010) A synchronized quorum of genetic clocks. *Nature 463*, 326–330.

12. Slotine, J. J., and Li, W. *Applied nonlinear control*; Prentice-hall Englewood Cliffs, NJ, 1991; Vol. 199.

13. Bennett, M. R., Pang, W. L., Ostroff, N. A., Baumgartner, B. L., Nayak, S., Tsimring, L. S., and Hasty, J. (2008) Metabolic gene regulation in a dynamically changing environment. *Nature 454*, 1119–1122.

14. Elowitz, M. B., Levine, A. J., Siggia, E. D., and Swain, P. S. (2002) Stochastic gene expression in a single cell. *Science 297*, 1183–1186.

15. Swain, P. S., Elowitz, M. B., and Siggia, E. D. (2002) Intrinsic and extrinsic contributions to stochasticity in gene expression. *Proceedings of the National Academy of Sciences 99*, 12795–12800.

16. Fiore, G., Menolascina, F., di Bernardo, M., and di Bernardo, D. (2013) An experimental approach to identify dynamical models of transcriptional regulation in living cells. *Chaos: An Interdisciplinary Journal of Nonlinear Science 23*, 025106–025106.

17. Ferry, M., Razinkov, I., and Hasty, J. (2011) Microfluidics for synthetic biology from design to execution. *Methods Enzymol 497*, 295.

18. Morari, M., and Lee, J. H. (1999) Model predictive control: past, present and future. *Computers & Chemical Engineering 23*, 667–682.

19. Fossas, E., Grinó, R., and Biel, D. (2001) Quasi-Sliding control based on pulse width modulation, zero averaged dynamics and the L2 norm. *Advances in Variable Structure System, Analysis, Integration and Applications* 335–344.

20. D'Amico, M. B., and Angulo, F. (2013) Performance of a Zero Average Dynamics-controlled buck converter using different pulse-width modulation schemes. *International Journal of Circuit Theory and Applications*

21. Lang, G. I., and Botstein, D. (2011) A Test of the Coordinated Expression Hypothesis for the Origin and Maintenance of the GAL Cluster in Yeast. *PloS one 6*, e25290.

22. Golberg, D. E. (1989) Genetic algorithms in search, optimization, and machine learning. *Addion wesley 1989*.

23. Ramos, R. R., Biel, D., Fossas, E., and Guinjoan, F. (2003) A fixed-frequency quasi-sliding control algorithm: application to power inverters design by means of FPGA implementation. *Power Electronics, IEEE Transactions on 18*, 344–355.

Figure Legends

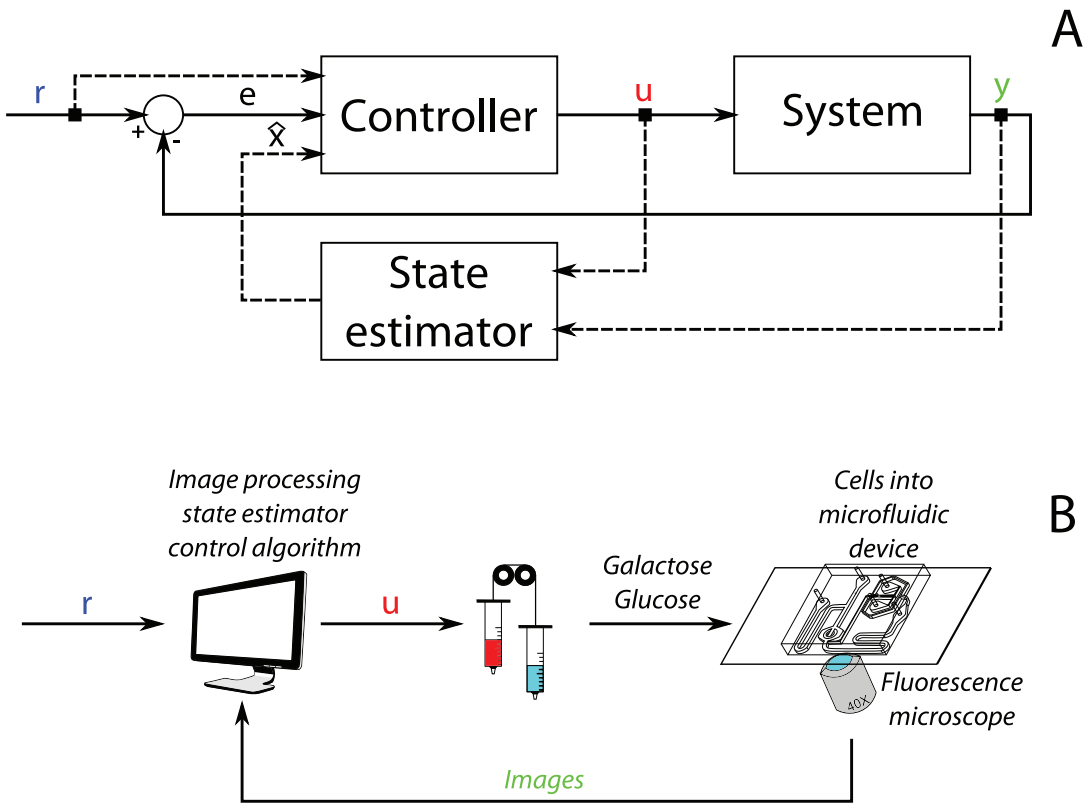

Figure 1: **Control scheme and experimental set-up.** (A) Generalised control scheme used to implement PI, MPC and ZAD regulators. In the case of model-free regulators (e.g. PI), the control error e (namely the difference in between the control reference r and the system's output y) is minimised by the controller calculating the control input u. Model-based controllers, i.e. MPC and ZAD, use not only the control error e but also the dynamical model of the *GAL1* promoter in the State estimator block. (B) Experimental set-up: a PC governs the entire platform running an algorithm that during each sampling interval: *(i)* processes the images acquired by the microscope to calculate the output y, *(ii)* runs the state estimator (when needed) and the control algorithms to calculate the input u for the next sampling interval. *(iii)* controls the automated syringes so as to provide the calculated input to the cells.

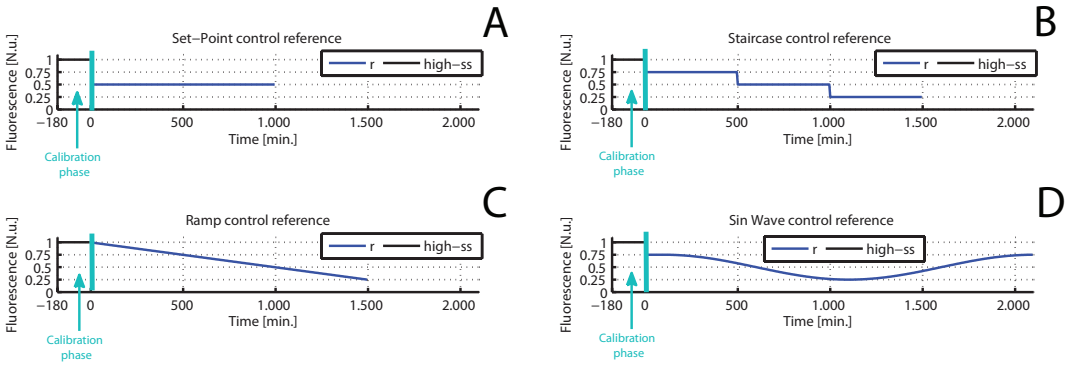

Figure 2: **Reference signals for set-point and tracking control tasks.** (A) The desired set-point r (**blue line**) is equal to 50% of the average fluorescence measured during the initial calibration phase of 180 min (**black line**) (B) The desired level of fluorescence (r) is a three-step descending staircase signal, each step is set at a given percentage (75%, 50% and 25%) of the average fluorescence measured during the initial calibration phase of 180 min. (C) The desired level of fluorescence (r) is a linear descending ramp starting at 100% of the average fluorescence measured during the initial calibration phase of 180 min and going down to 25%. (D) The desired level of fluorescence (r) is a steady state signal equal to 75% of the average fluorescence measured during the calibration phase, with a duration of 100 min; followed by a sinusoidal wave of period $T = 2000$ min defined as $s(t) = 0.5 + 0.25 \sin\left(\frac{2\pi}{T}(t - 100) + \frac{\pi}{2}\right)$

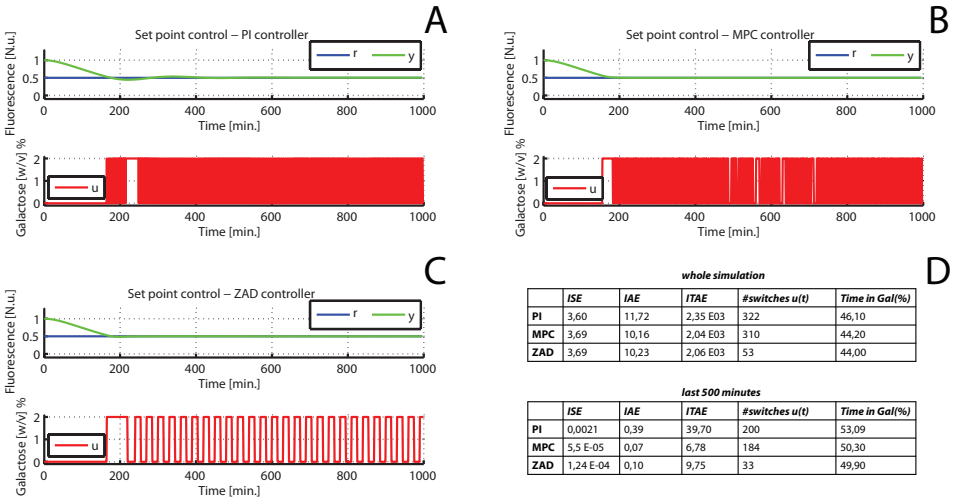

whole simulation

	ISE	*IAE*	*ITAE*	*#switches u(t)*	*Time in Gal(%)*
PI	3,60	11,72	2,35 E03	322	46,10
MPC	3,69	10,16	2,04 E03	310	44,20
ZAD	3,69	10,23	2,06 E03	53	44,00

last 500 minutes

	ISE	*IAE*	*ITAE*	*#switches u(t)*	*Time in Gal(%)*
PI	0,0021	0,39	39,70	200	53,09
MPC	5,5 E-05	0,07	6,78	184	50,30
ZAD	1,24 E-04	0,10	9,75	33	49,90

Figure 3: ***In-silico* set-point control task**. The blue line is the reference signal (r). The green line is the simulated fluorescence level (y). The red line is the control input (u). (A-C) Three *in-silico* set-point control experiments performed on the *GAL1* promoter mathematical model by the means of the PI (A), MPC (B) and ZAD (C) controllers . The initial level of fluorescence is assumed to be equal to 1. The control action starts at time $t = 0$ min and ends at $t = 1000$ min. (D) Performance indices: Integral Square Error (ISE), Integral Absolute Error (IAE), Integral Time Absolute Error (ITAE), number of switches of the control input, and the percentage of time during which the model is provided with the 'ON' input.

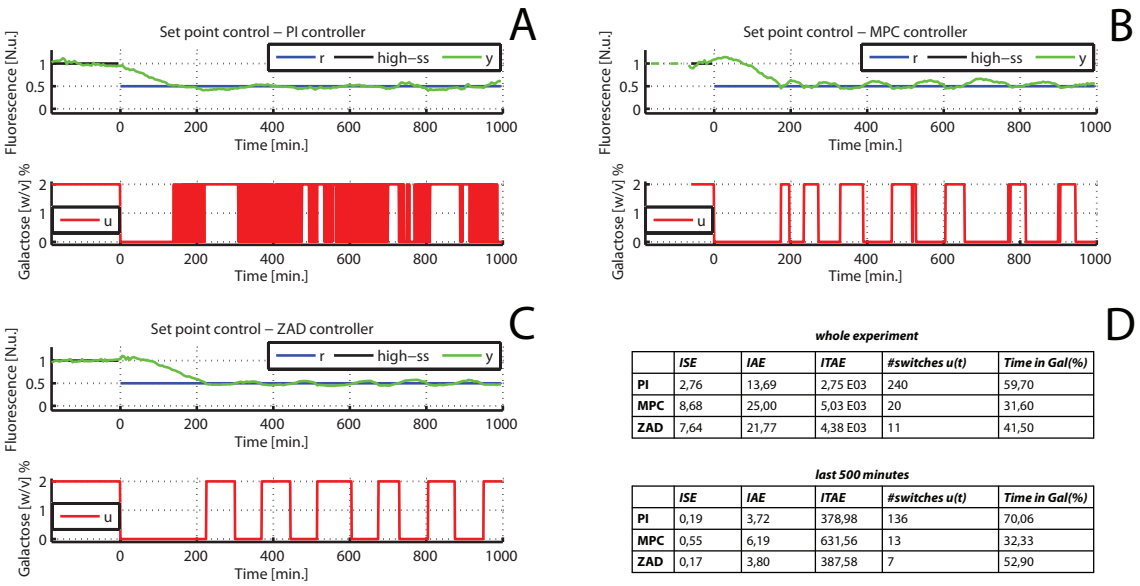

whole experiment

	ISE	*IAE*	*ITAE*	*#switches u(t)*	*Time in Gal(%)*
PI	2,76	13,69	2,75 E03	240	59,70
MPC	8,68	25,00	5,03 E03	20	31,60
ZAD	7,64	21,77	4,38 E03	11	41,50

last 500 minutes

	ISE	*IAE*	*ITAE*	*#switches u(t)*	*Time in Gal(%)*
PI	0,19	3,72	378,98	136	70,06
MPC	0,55	6,19	631,56	13	32,33
ZAD	0,17	3,80	387,58	7	52,90

Figure 4: ***In-vivo* set-point control task**. The black line is the average fluorescence intensity during the calibration phase of 180 min. The blue line is the reference signal (r). The green line is the measured fluorescence level (y) across the yeast population. The red line is the control input (u). (A-C) Three *in-vivo* set-point control experiments by the means of the PI (A), MPC (B) and ZAD (C) controllers. The control action starts at time $t = 0$ min and ends at $t = 1000$ min. (D) Performance indices: Integral Square Error (ISE), Integral Absolute Error (IAE), Integral Time Absolute Error (ITAE), number of switches of the control input, and the percentage of time during which the model is provided with the 'ON' input.

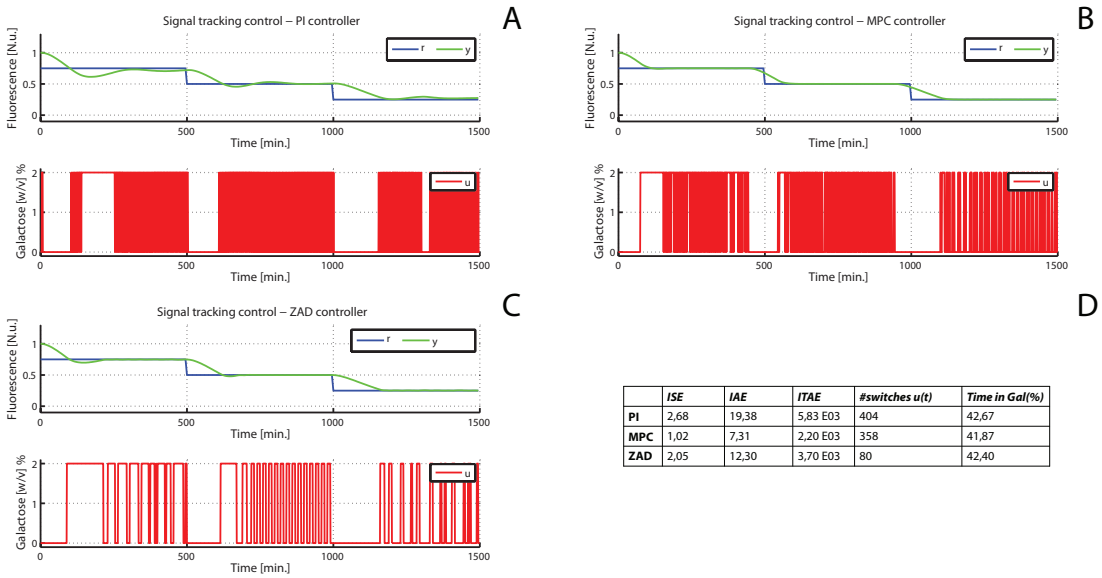

	ISE	IAE	ITAE	#switches u(t)	Time in Gal(%)
PI	2,68	19,38	5,83 E03	404	42,67
MPC	1,02	7,31	2,20 E03	358	41,87
ZAD	2,05	12,30	3,70 E03	80	42,40

Figure 5: ***In-silico* staircase tracking control task**. The blue line is the reference signal (r). The green line is the simulated fluorescence level (y). The red line is the control input (u). (A-C) Three *in-silico* staircase tracking control experiments performed on the *GAL1* promoter mathematical model by the means of the PI (A), MPC (B) and ZAD (C) controllers. The initial level of fluorescence is assumed to be equal to 1. The control action starts at time $t = 0$ min and ends at $t = 1000$ min. (D) Performance indices: Integral Square Error (ISE), Integral Absolute Error (IAE), Integral Time Absolute Error (ITAE), number of switches of the control input, and the percentage of time during which the model is provided with the 'ON' input.

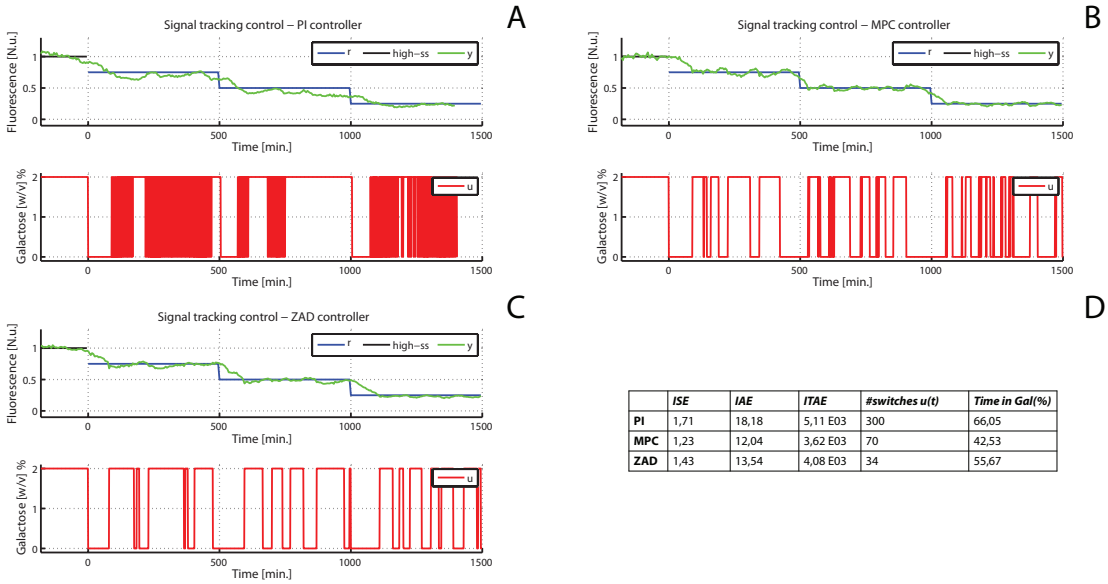

	ISE	IAE	ITAE	#switches u(t)	Time in Gal(%)
PI	1,71	18,18	5,11 E03	300	66,05
MPC	1,23	12,04	3,62 E03	70	42,53
ZAD	1,43	13,54	4,08 E03	34	55,67

Figure 6: ***In-vivo* staircase tracking control task**. The black line is the average fluorescence intensity during the calibration phase of 180 min. The blue line is the reference signal (r). The green line is the measured fluorescence level (y) across the yeast population. The red line is the control input (u). (A-C) Three *in-vivo* staircase tracking control experiments by the means of the PI (A), MPC (B) and ZAD (C) controllers. The control action starts at time $t = 0$ min and ends at $t = 1000$ min. (D) Performance indices: Integral Square Error (ISE), Integral Absolute Error (IAE), Integral Time Absolute Error (ITAE), number of switches of the control input, and the percentage of time during which the model is provided with the 'ON' input.

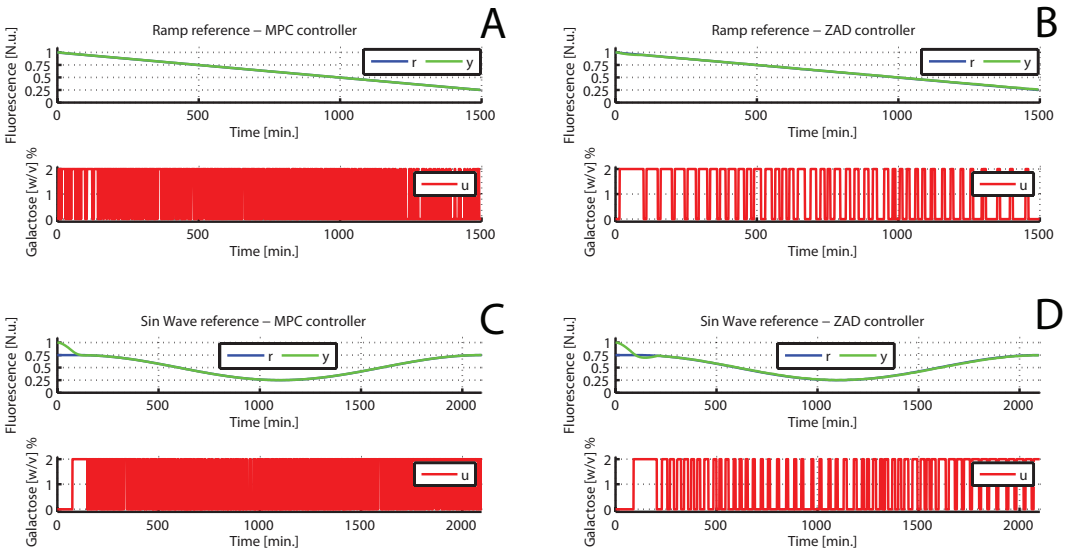

E

Ramp reference

	ISE	*IAE*	*ITAE*	*#switches u(t)*	*Time in Gal(%)*
MPC	1,50 E-03	0,64	192,33	462	51,87
ZAD	4,50 E-03	0,79	236,50	86	51,07

Sin Wave reference

	ISE	*IAE*	*ITAE*	*#switches u(t)*	*Time in Gal(%)*
MPC	0,60	4,39	1,84 E03	610	49,62
ZAD	0,56	4,41	1,85 E03	105	49,24

Figure 7: ***In-silico* ramp and sin wave tracking control tasks**. The blue line is the reference signal (r). The green line is the simulated fluorescence level (y). The red line is the control input (u). (A-B) Two *in-silico* ramp tracking control experiments performed on the *GAL1* promoter mathematical model by the means of the MPC (A) and ZAD (B) controllers. The initial level of fluorescence is assumed to be equal to 1. The control action starts at time $t = 0$ min and ends at $t = 1500$ min. (C-D) Two *in-silico* sin wave tracking control experiments performed on the *GAL1* promoter mathematical model by the means of the MPC (C) and ZAD (D) controllers. The initial level of fluorescence is assumed to be equal to 1. The control action starts at time $t = 0$ min and ends at $t = 2100$ min. (E) Performance indices: Integral Square Error (ISE), Integral Absolute Error (IAE), Integral Time Absolute Error (ITAE), number of switches of the control input, and the percentage of time during which the model is provided with the 'ON' input.

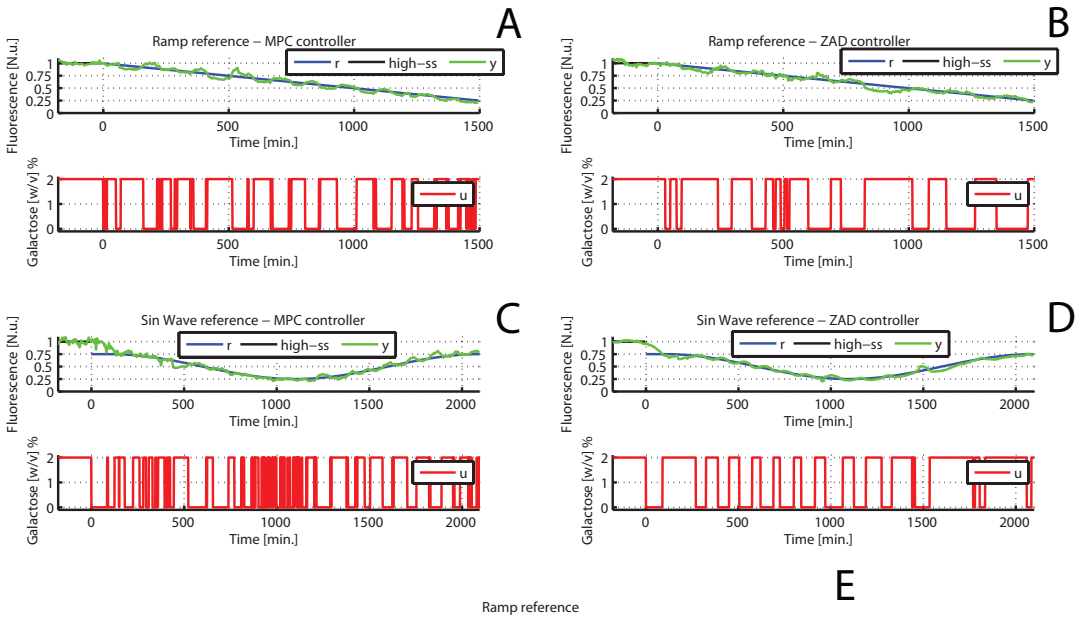

E

Ramp reference

	ISE	*IAE*	*ITAE*	*#switches u(t)*	*Time in Gal(%)*
MPC	0,75	12,76	3,84 E03	71	54,27
ZAD	0,78	12,19	3,67 E03	24	55,00

Sin Wave reference

	ISE	*IAE*	*ITAE*	*#switches u(t)*	*Time in Gal(%)*
MPC	1,84	17,26	7,27 E03	127	46,90
ZAD	0,98	15,02	6,32 E03	29	59,05

Figure 8: ***In-vivo* ramp and sin wave tracking control tasks.** The black line is the average fluorescence intensity during the calibration phase of 180 min. The blue line is the reference signal (r). The green line is the measured fluorescence level (y) across the yeast population. The red line is the control input (u). (A-B) Two *in-vivo* ramp tracking control experiments by the means of the MPC (A) and ZAD (B) controllers. The control action starts at time $t = 0$ min and ends at $t = 1500$ min. (C-D) Two *in-vivo* sin wave tracking control experiments by the means of the MPC (C) and ZAD (D) controllers. The control action starts at time $t = 0$ min and ends at $t = 2100$ min. (E) Performance indices: Integral Square Error (ISE), Integral Absolute Error (IAE), Integral Time Absolute Error (ITAE), number of switches of the control input, and the percentage of time during which the model is provided with the 'ON' input.